e-ISSN: 2550-164X

Available online at
https://jmeche.uitm.edu.my/

Journal of Mechanical Engineering 23(2) 2026, 135 – 150.

Journal of Mechanical Engineering

Synthesis of Graphene Quantum Dots from Rice Husk for Water Treatment Applications

Faiz Haikal Johari[1], Siti Rabizah Makhsin[1*], Azib Haiman Roslan[1], Syazwani Mohd Zaki[2], Beenish Siddique[3]

[1]*Nanomaterials for Sensors and Heat Transfer, Faculty of Mechanical Engineering, Universiti Teknologi MARA, 40450 Shah Alam, Selangor*

[2]*Department of Manufacturing and Materials Engineering, Kulliyah of Engineering, International Islamic University Malaysia, PO Box 50728 Kuala Lumpur, Malaysia*

[3]*AEH Innovative Hydrogel Ltd, Graphene Engineering Innovation Centre, Sackville St, Manchester M1 3BB, United Kingdom*

ARTICLE INFO

Article history:
Received 12 November 2025
Revised 1 April 2026
Accepted 16 April 2026
Online first
Published 15 May 2026

Keywords:
Graphene quantum dots
Boiling method
Rice husk
Heavy metal purification
Biomass

DOI:
10.24191/jmeche.v23i2.11759

ABSTRACT

This study aims to develop a sustainable method for synthesizing graphene quantum dots (GQDs) from biomass waste for water treatment applications. Rice husk, a carbon-rich waste material, was used as a precursor for GQDs synthesis via a simple boiling method, providing a sustainable and cost-effective approach. The optimal GQDs sample (2.5% w/v) was prepared from 5 g of rice husk and 200 mL of deionized water, exhibiting greenish fluorescence under UV light, indicating successful GQD formation. The synthesized GQDs were characterized by ultraviolet–visible (UV–Vis), Fourier-transform infrared (FTIR) and fluorescence spectroscopy, as well as zeta potential analysis. The 2.5% w/v filtered GQDs showed low absorption beyond 230 nm in the UV region, a zeta potential of −20.6 ± 1.0 mV indicating good colloidal stability, and the presence of oxygen-containing functional groups that enhance adsorption capability, as confirmed by FTIR analysis. The adsorption performance of GQDs was evaluated using methylene blue (an organic dye) and copper ions (a heavy metal). The electrical conductivity (EC) of the copper sulphate ($CuSO_4$) solution decreased by 54.2%, demonstrating significant removal of copper ions. In contrast, the EC of the methylene blue solution increased slightly by 21.5%, possibly due to the release of smaller ionic species during degradation or interactions between GQDs and dye molecules. In summary, this study presents an eco-friendly approach for converting biomass waste into functional nanomaterials for water purification, contributing to sustainable waste management and clean water initiatives aligned with the United Nations Sustainable Development Goals (SDGs).

[1*] Corresponding author. *E-mail address*: sitirabizah@uitm.edu.my
https://doi.org/10.24191/jmeche.v23i2.11759

INTRODUCTION

Water contamination by heavy metals and organic dyes remains a pressing global issue, posing significant threats to both environmental and human health (Thakur et al., 2026). Conventional treatment methods often struggle to effectively remove these contaminants, highlighting the need for more efficient and sustainable water purification strategies. Among materials exhibiting strong interactions with heavy metal ions, graphene quantum dots (GQDs) have attracted significant attention due to their unique optical and structural properties, high surface area, and tunable surface chemistry (Shtepliuk et al., 2017). These characteristics enable their application in rapid and sensitive detection, cost-effective production, and efficient removal of heavy metal pollutants from water.

Recently, the use of biomass for synthesizing graphene-based materials has attracted considerable interest due to their high carbon content and abundant availability (Boran et al., 2026). This approach enables the production of graphene-based materials through green, cost-effective processes (Saleem et al., 2023). In Malaysia, biomass generation exceeded 100 million tons in 2020 and is projected to reach 1,200 million tons by 2035 (Rusli et al., 2024). This increased availability provides a sustainable, renewable source of organic carbon for the synthesis of graphene-based nanomaterials. Among various biomass resources in Malaysia, including rice husks, oil palm biomass, sago biomass, wood residues, coconut husks, and sugarcane residues (Rusli et al., 2024), rice husk is particularly attractive due to its high carbon and silica content. As a major rice-producing country, Malaysia generates substantial quantities of rice husk as a byproduct of its milling industry, ensuring a continuous and abundant supply. The use of rice husk for GQDs synthesis offers a sustainable approach to valorizing agricultural waste that would otherwise contribute to environmental pollution through open burning or landfilling. Moreover, rice husk can be converted into GQDs using established synthesis methods, such as hydrothermal processing (Chai et al., 2019) and electrochemical or green synthesis approaches (Bressi et al., 2021). However, existing synthesis methods often require high energy input, long processing times, or toxic reagents, limiting their scalability and sustainability. Therefore, developing a simple, low-cost, and environmentally benign synthesis route remains a critical challenge.

More recently, microwave-assisted synthesis has emerged as an efficient method for producing GQDs, enabling rapid conversion of carbonaceous materials into nanostructured forms (Cui et al., 2024; Roslan et al., 2025). In this process, the precursor is exposed to microwave radiation, resulting in rapid and uniform heating that facilitates the breakdown of bulk carbon into nanoscale GQDs. This method enables the formation of smaller, more uniform nanoparticles with enhanced photoluminescence (Zhu et al., 2021). Citric acid is commonly used as a precursor due to its well-defined molecular structure and predictable carbonization behaviour under microwave irradiation, yielding high-quality GQDs (More et al., 2018; Dong et al., 2012).

In the present study, rice husk was converted into GQDs using two approaches: ethanol extraction and direct boiling. In the ethanol extraction route, microwave-assisted heating was further employed to facilitate the formation of quantum dot-sized particles. The synthesized GQDs were subsequently applied for the treatment of contaminated water using methylene blue (MB) as a model organic dye (Yin et al., 2021) and copper (II) sulfate ($CuSO_4$) as a representative heavy metal contaminant (National Research Council, 2000). Changes in visual appearance and electrical conductivity (EC) were evaluated to assess the effectiveness of the GQDs in water purification.

https://doi.org/10.24191/jmeche.v23i2.11759

METHODOLOGY

Materials

The materials required for synthesizing GQDs from biomass were rice husk (NSR AgroGarden), ultrapure deionized water (DI water, 18.2 MΩ·cm, Millipore at 25°C), absolute ethanol (≥99.8%, Merck), and distilled water. For the application of wastewater treatment, the chemicals required were copper (II) sulphate ($CuSO_4$) (99%), and methylene blue (MB); $C_{16}H_{18}ClN_3S$ (≥82%, Fish & Furry Friends). All materials were exquisitely applied to perform experiments without any purification.

Synthesis of GQD via rice husk

In synthesizing GQDs from rice husk, two approaches were used: the ethanol extraction method and the boiling method, both of which break the silica barrier and remove unwanted byproducts. Hence, high-purity carbon can be extracted from the rice husks. The parameters involved in synthesizing GQDs are summarised in Table 1.

Table 1. Summary of synthesis parameters of GQDs

Synthesis Method	Sample ID	Type of Carbon Precursor	Amount of Precursor (g)	Type of Solvent	Total Conc. (%w/v)	Filter Status
Ethanol Extraction	n/a	Rice husk	10.0	Ethanol	10.0	Filtered
Boiling Method	A	Rice husk	5.0	DI water	2.5	Unfiltered
	B		5.0		2.5	Filtered
	C		10.0		10.0	Unfiltered
	D		10.0		10.0	Filtered
	E		12.5		12.5	Unfiltered
	F		12.5		12.5	Filtered

Synthesis of GQD via rice husk

In this work, the ethanol extraction method adapted from previous studies (Saleem et al., 2023; Dong et al., 2012) was employed, with dry date palm tree leaves replaced by rice husks as the carbon precursor. The process began by dispersing 10 g of rice husks in 100 mL of ethanol, then stirring continuously at room temperature for 4 h to extract organic compounds. The mixture was subsequently centrifuged at 8000 rpm for 10 min to separate solid residues. The precipitate was discarded, and the supernatant was filtered to remove any remaining particles. The resulting clear solution was then concentrated using a rotary evaporator. Subsequently, 50 mL of distilled water was added to the concentrated extract to facilitate further processing, followed by microwave heating for 10–14 min to induce carbonization and form nanoscale structures. After heating, the mixture was filtered using a 0.22 μm syringe filter to remove residual impurities, and the final filtrate was dried to obtain the GQDs product, as illustrated in Fig. 1.

Boiling method

In this work, an alternative approach for extracting carbon from biomass was adapted from previous work (Saleem et al., 2023), in which dry date palm leaves were replaced with rice husks as the carbon precursor. The overall process is illustrated in Fig. 2. GQDs were synthesized via a boiling method using rice husks as a precursor at three concentrations (2.5–12.5% w/v) to investigate the effect of precursor loading on GQD formation. Specifically, 5 g in 200 mL produced a dilute system (2.5% w/v), while 10 g and 12.5 g in 100 mL yielded higher concentrations of 10% and 12.5% w/v, respectively.

https://doi.org/10.24191/jmeche.v23i2.11759

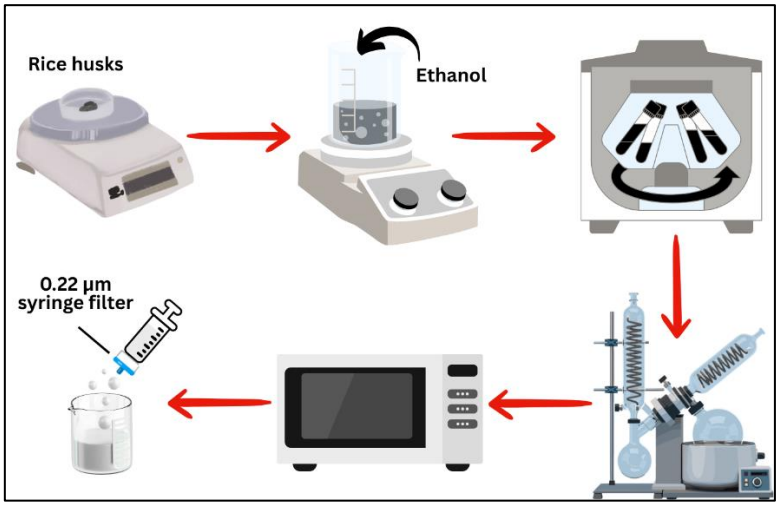

Fig. 1. Preparation of GQDs from rice husks using the ethanol extraction method.

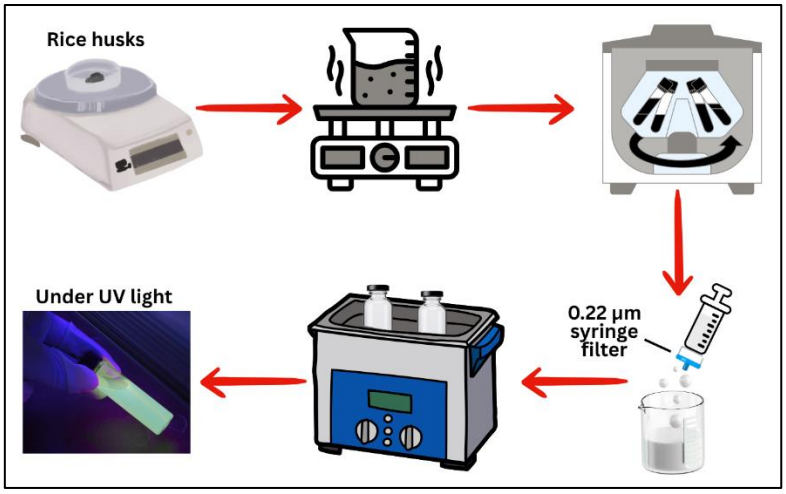

Fig. 2. Preparation of GQDs from rice husks using the boiling method.

For the first concentration, 5 g of rice husks was dispersed in 200 mL of DI water. The mixture was heated at 80 °C under continuous stirring at 350 rpm for 2 h. After cooling to room temperature, the mixture was centrifuged at 6000 rpm for 10–15 min to separate the solid residue. The resulting supernatant was divided into two portions. One portion was filtered using a 0.22 µm syringe filter, while the other was retained without filtration. Both samples were subsequently subjected to ultrasonication in a water bath for 30 min to promote uniform dispersion and enhance nanoscale structuring. The samples were then examined under UV illumination to observe fluorescence, indicating the possible formation of GQDs. The procedure was repeated for higher precursor concentrations using 10 g and 12.5 g of rice husks, each dispersed in 100 mL of DI water. The parameters investigated are summarized in Table 1.

https://doi.org/10.24191/jmeche.v23i2.11759

Characterization of GQDs

UV-Vis spectroscopy (JASCO, V-670 UV-Vis-NIR Spectrophotometer) was used to determine the sample's optical properties over a scan range of 200-1000 nm. Each sample was measured in absorption mode at room temperature, with a quartz-type cuvette filled with DI water as the standard. Next, the functional groups and chemical bonds in GQDs were identified using Fourier-transform infrared (FTIR) spectroscopy. Then, all the samples were also analyzed for Zeta Potential (Malvern Nanoseries Model ZEN3600) to assess the dispersity and stability of GQDs, while the photoluminescence (PL) properties and the specific emission peak(s) of GQDs were measured using a Fluorescence Spectrometer F-2700.

Application of GQDs in wastewater treatment

The synthesized GQDs were evaluated for their potential in wastewater treatment, focusing on their efficiency in removing both organic dyes and heavy metal ions from contaminated water. MB was used as a model organic contaminant, while $CuSO_4$ was selected as the representative heavy metal. For the heavy metal test, $CuSO_4$ was prepared at a concentration of 1.3 mg/L (Fig. 3(a)), corresponding to the Maximum Contaminant Level (MCL) for copper in drinking water, as defined by water quality standards (National Research Council, 2000). For the organic contaminant test, MB was prepared at a concentration of 0.2 mg/L in tap water. Each contaminated solution was treated with the synthesized GQDs and incubated for 1 h. Changes in the solutions' visual appearance were recorded. The electrical conductivity (EC) of each sample was measured before and after treatment at room temperature using an HM Digital AP-2 EC meter. Measurements were conducted in triplicate (n = 5) to obtain reliable average values. Finally, the optical properties of the treated samples were analyzed using UV–Vis spectroscopy to evaluate changes in absorbance associated with MB and $CuSO_4$ following GQDs treatment.

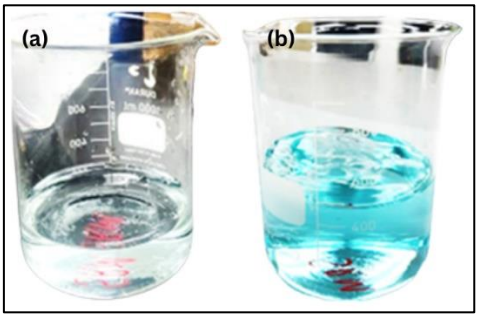

Fig. 3. The solution of (a) 1.3 mg/L of $CuSO_4$ and (b) 0.2 mg/L of MB.

RESULTS AND DISCUSSION

Characterization of synthesized GQDs

In the ethanol-extraction synthesis of GQDs from rice husks, the supernatant was rotary-evaporated to remove ethanol, yielding a carbon-rich solution prior to microwave processing. According to previous work (Saleem et al., 2023), this step is expected to produce a semi-solid slurry, indicating successful extraction of carbonaceous material. However, in the present study, the post-evaporation solution remained completely clear, with no visible residue or slurry formation observed. The procedure was repeated three times under identical conditions, yet the outcome remained unchanged. This suggests that the extracted compounds were either too dilute or that the evaporation process led to the loss of volatile organic

https://doi.org/10.24191/jmeche.v23i2.11759

components, possibly due to over-evaporation. As a result, the expected intermediate product for subsequent carbonization was not obtained.

In contrast, the synthesis of GQDs via the boiling method was successful. The optical properties of the synthesized samples were evaluated under UV illumination (365 nm). All samples exhibited greenish-blue fluorescence, as summarized in Table 2. Specifically, the filtered GQDs at concentrations of 2.5%, 10%, and 12.5% w/v (Samples B, D, and F) and the unfiltered GQDs at 2.5% w/v (Sample A) displayed strong green fluorescence. In contrast, the unfiltered samples at higher concentrations (10% and 12.5% w/v; Samples C and E) exhibited weak, cloudy, or negligible fluorescence under UV light.

Table 2. The synthesized GQDs observed under visible light and UV light from (a) to (f) using the boiling method from rice husks; 2.5% w/v with (a) unfiltered and (b) filtered, 10% w/v with (c) unfiltered and (d) filtered, 12.5% w/v with (e) unfiltered and (f) filtered GQDs

Sample ID	Sample A	Sample B	Sample C	Sample D	Sample E	Sample F
Under visible light						
Under UV light						

UV–Vis spectroscopy measures the absorption or reflection of light in the ultraviolet and visible regions of the electromagnetic spectrum. This technique utilizes light in the visible, near-ultraviolet, and near-infrared ranges. The colour of a substance is directly related to its absorption and reflection characteristics within the visible spectrum. As shown in Fig. 4, the absorbance intensity increased with increasing concentration, indicating higher optical density and enhanced light–matter interaction due to the greater nanoparticle content (Moresi & Parente, 2014).

The fluorescence behaviour of the synthesized GQDs was analyzed using excitation and emission spectroscopy. The excitation spectrum exhibits a prominent peak at approximately 447 nm, indicating the optimal excitation wavelength, as shown in Fig. 5. Upon excitation at this wavelength, a photoluminescence (PL) emission peak was observed at 513.03 nm (red line in Fig. 5), corresponding to green emission in the visible region. This emission peak is consistent with previously reported values, confirming the successful synthesis of GQDs with characteristic photoluminescent properties (Piotrowski et al., 2024). From the PL spectra, Sample B exhibited the highest emission intensity, followed by Samples F and D. In contrast, the PL intensity of unfiltered samples decreased with increasing concentration. This observation indicates that the filtration process enhances the photoluminescence performance of GQDs. The presence of larger aggregates or residual particulate matter can promote non-radiative recombination pathways, leading to energy dissipation and reduced emission intensity. Therefore, the removal of these components enables a

https://doi.org/10.24191/jmeche.v23i2.11759

stronger contribution from well-dispersed, highly emissive GQDs, consistent with previous findings (Zhu et al., 2021).

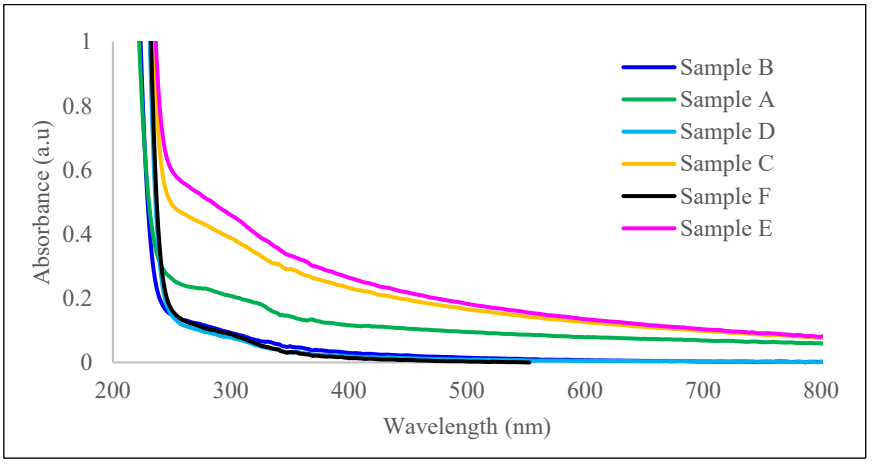

Fig. 4. UV-Vis results for the synthesized GQDs using the boiling method from rice husks.

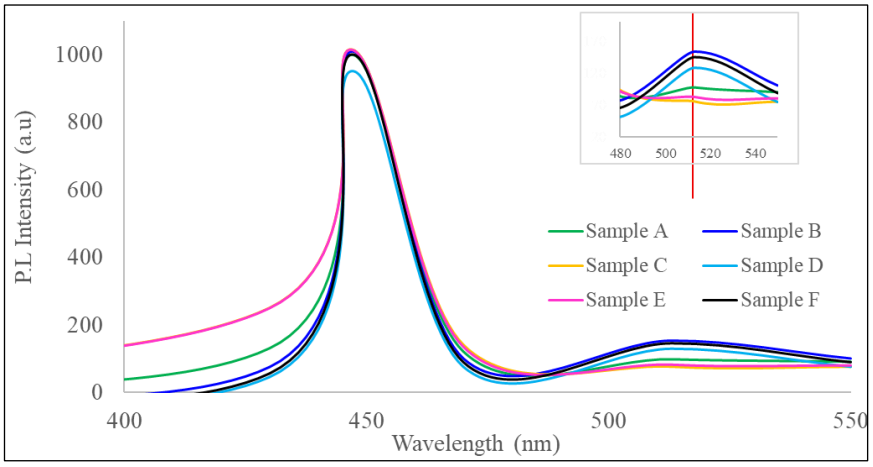

Fig. 5. PL emission of synthesized GQDs with an inset showing the zoomed-in range between 480 nm to 550 nm at the highest emission peaks (red line).

Zeta potential analysis was performed to evaluate the colloidal stability of synthesized GQDs under varying precursor concentrations and filtration conditions. A colloidal system is generally considered stable when the zeta potential is more negative than −20 mV (Hong et al., 2020). In this study, the zeta potential values of the synthesized GQDs are summarized in Table 3. Each measurement was conducted in triplicate, and the most representative value was selected based on consistency among the readings. The results show that Samples A, B, C, E, and F exhibited zeta potential values ranging from −20.0 to −24.0 mV, indicating moderately high colloidal stability. Notably, Samples C and D were both prepared at a concentration of 10% w/v; however, Sample D exhibited a less negative zeta potential (−15.93 mV) compared to Sample C.

https://doi.org/10.24191/jmeche.v23i2.11759

This suggests that the filtration process may have altered the particle size distribution and surface charge density, thereby reducing the colloidal system's electrostatic stability.

Table 3. Zeta potential and zeta size measurement for synthesized GQDs

GQDs Sample ID	Total Concentration (% w/v)	Filter Status	Zeta Potential (mV)
A	2.5	unfiltered	–20.50 ± 2.38
B	2.5	filtered	–20.60 ± 1.00
C	10	unfiltered	–23.57 ± 1.00
D	10	filtered	–15.93 ± 0.37
E	12.5	unfiltered	–21.63 ± 0.63
F	12.5	filtered	–21.57 ± 1.75

The chemical bonding states of the synthesized GQDs were analyzed using Fourier-transform infrared (FTIR) spectroscopy. This technique provides information on molecular vibrations and functional groups, making it a valuable tool for identifying chemical structures and surface functionalities (Marie & Torbjorn, 2007). As shown in Fig. 6, the FTIR spectra of the filtered samples (B, D, and F) exhibit consistent characteristic peaks, indicating uniform surface chemistry and robustness of the GQDs functional groups. A broad, intense absorption band observed in the 3200–3400 cm^{-1} range is attributed to O–H stretching vibrations from hydroxyl groups and adsorbed water, confirming the hydrophilic nature of the GQDs. The presence of aliphatic C–H stretching vibrations is indicated by peaks in the range of 2800–3000 cm^{-1}, corresponding to sp^3-hybridised carbon structures. Additionally, a prominent absorption band observed between 1400 and 1600 cm^{-1} is attributed to aromatic C=C stretching from the graphitic domains and C=O stretching from carbonyl, carboxyl, or quinone functional groups. These features confirm the presence of oxygen-containing functional groups and a partially graphitized carbon structure.

For the unfiltered samples (A, C, and E), a broader, more intense O–H stretching band in the 3200–3600 cm^{-1} range was observed, indicating a higher degree of surface hydroxylation and adsorbed moisture. Peaks in the 2800–3000 cm^{-1} region further confirm the presence of aliphatic C–H bonds. The absorption band in the 1400–1700 cm^{-1} range corresponds to overlapping contributions from aromatic C=C and C=O stretching vibrations, suggesting a graphitic core decorated with oxygen-containing functional groups. These functional groups not only confirm the chemical structure of GQDs but also enhance their hydrophilicity, facilitating dispersion in aqueous media and providing active sites for adsorption and further functionalization.

Evaluation of wastewater treatment

GQD samples A, B, D, and F were selected for wastewater treatment applications based on their preliminary characterization results. The presence of MB in water produces a distinct blue colour, whereas $CuSO_4$ solution appears light blue. To evaluate the adsorption performance of the synthesized GQDs, the contaminated solutions were treated at a 1:1 volume ratio. Specifically, 5 mL of each contaminated solution was mixed with 5 mL of the GQDs solution. All selected samples (A, B, D, and F) exhibited similar visual changes upon treatment. As shown in Table 4, both MB and $CuSO_4$ solutions became colourless after treatment, indicating effective removal of the contaminants. The disappearance of the characteristic blue colour indicates a strong interaction between GQDs and contaminants, demonstrating their potential to remove both organic dyes and heavy metal ions from aqueous systems.

https://doi.org/10.24191/jmeche.v23i2.11759

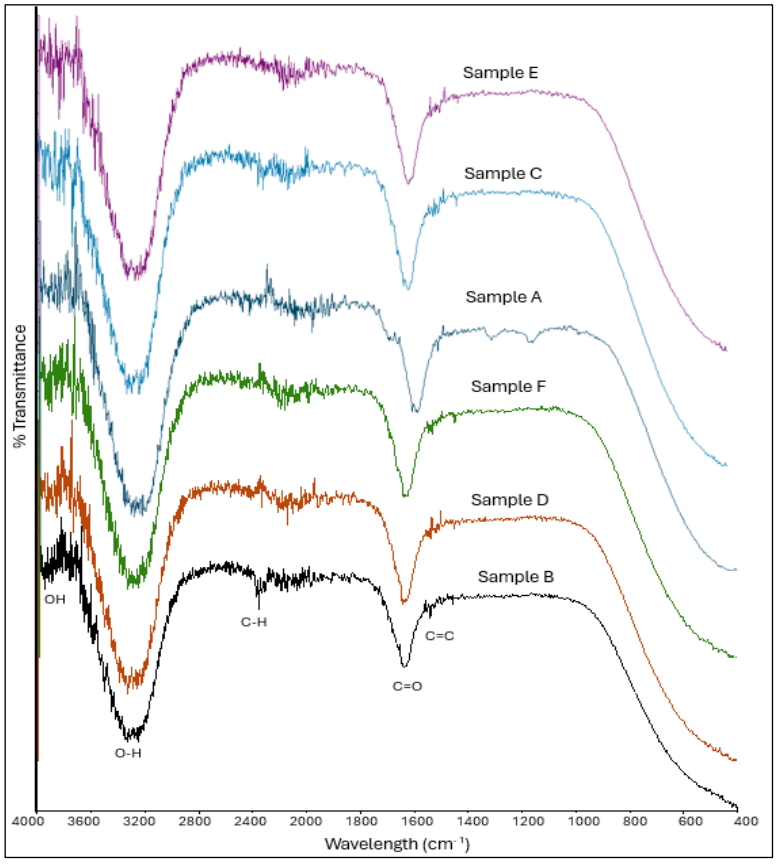

Fig. 6. FTIR results for the GQDs samples A, B, C, D, E, and F.

EC measurements were conducted to evaluate the ionic content of the solutions and to assess the reduction of heavy metal ions, specifically in $CuSO_4$ solutions, following treatment with GQDs. EC readings were recorded before and after treatment to determine changes in conductivity. For reference, laboratory tap water had an EC of 103 µS/cm, while DI water had a significantly lower EC of 5 µS/cm. The contaminated samples displayed varying initial EC values, as summarized in Table 5.

Although decolourization of the methylene blue (MB) solution was successfully achieved, an increase in electrical conductivity (EC) was observed after treatment with GQDs (Fig. 7). All samples exhibited significantly higher post-treatment EC values compared to the initial value of 107 µS/cm. This increase in EC is likely attributed to the release of ionic species from the GQDs surface, originating from residual synthesis byproducts or dissociable surface functional groups such as –COOH and –OH. These findings suggest that, despite GQDs' high capacity for dye removal, partial ion leaching may occur during treatment. Therefore, additional purification steps, such as dialysis or extensive washing, may be necessary to minimize the introduction of extraneous ions into the treated water.

https://doi.org/10.24191/jmeche.v23i2.11759

Table 4. The colour changes of 0.2 mg/L of MB and1.3 mg/L of CuSO4 after being added with GQDs samples A, B, D, and F

GQDs Sample	Treatment of 0.2 mg/L of MB		Treatment of 1.3 mg/L of $CuSO_4$	
	Before	After treatment with GQDs	Before	After treatment with GQDs
A				
B				
D				
F				

Table 5. Initial EC value for GQDs samples before and after mixing with MB and CuSO4. The % of EC changes counted based on the EC value after treatment vs the initial EC value of MB and CuSO4

Sample ID	Total concentration and EC of GQDs samples (After synthesized)		Treatment of MB (EC initial = 107 µS/cm)		Treatment of $CuSO_4$ (EC initial = 956 µS/cm)	
	Concentration (%w/v)	EC (µS/cm)	EC after (µS/cm)	% of EC changes	EC after (µS/cm)	% of EC changes
A	2.5 (Not filter)	156	330	+208.4	573	-40.1
B	2.5 (Filter)	135	130	+21.5	438	-54.2
D	10.0 (Filter)	516	534	+399.0	753	-21.2
F	12.5 (Filter)	582	673	+529.0	763	-20.2

https://doi.org/10.24191/jmeche.v23i2.11759

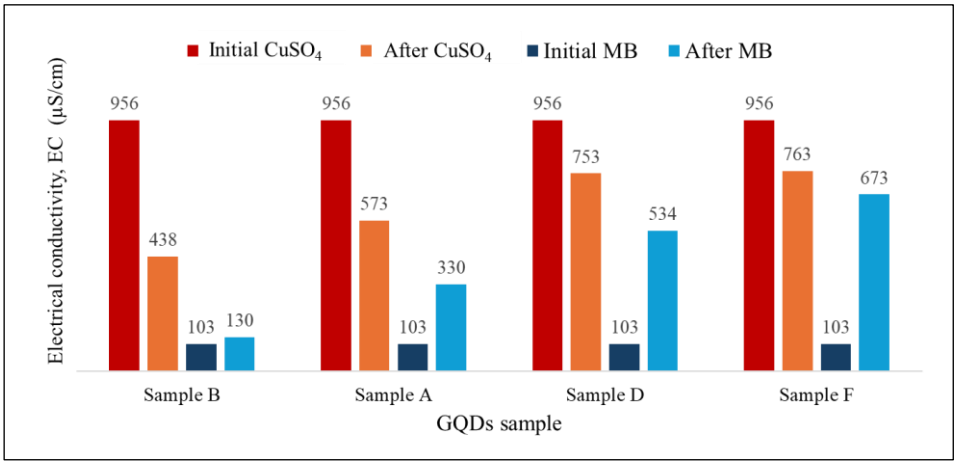

Fig. 7. The comparison EC measurement for both CuSO4 and MB before and after the addition of GQDs.

In contrast to the MB results, $CuSO_4$-contaminated water exhibited a different trend following treatment with GQDs. The initial EC of the $CuSO_4$ solution was 956 µS/cm. The most significant reduction was observed for Sample B, where the EC decreased to 438 µS/cm, indicating effective removal of Cu^{2+} ions. In comparison, higher GQDs concentrations (Samples D and F) resulted in less efficient removal, with final EC values of 753 and 763 µS/cm, respectively.

This reduced efficiency is likely due to particle agglomeration at higher concentrations, which limits the available surface area for ion adsorption. Sample A (2.5% w/v, unfiltered) exhibited a moderate EC reduction to 573 µS/cm, highlighting the role of filtration in enhancing GQDs performance. The typical permissible range for EC in drinking water is 200–800 µS/cm (Shahu et al., 2023). Overall, these results suggest that lower-concentration, well-purified rice husk-derived GQDs exhibit superior performance in heavy metal removal, whereas excessive concentration or insufficient purification adversely affect adsorption efficiency.

UV–Vis spectroscopy was further employed to analyze changes in absorbance associated with MB and $CuSO_4$ solutions after GQDs treatment, as shown in Fig. 8. For $CuSO_4$ (Fig. 8(b)), a characteristic absorption peak is typically observed at approximately 810 nm in aqueous solution (Rahardjo et al., 2018). A significant reduction in this peak after treatment indicates effective interaction and removal of Cu^{2+} ions by the GQDs. Additionally, all samples (A, B, D, and F) exhibited strong absorption in the range of 220–270 nm, attributed to π–π^* transitions of aromatic C=C bonds and C=O groups on the GQDs surface. Among these, Sample B showed the highest absorbance intensity, suggesting stronger surface interactions with Cu^{2+} ions and a higher degree of purity. This observation is consistent with the substantial EC reduction observed for this sample.

For MB (Fig. 8(c)), the characteristic absorption peak is typically observed at approximately 644 nm, in agreement with Yin et al. (2021). The disappearance or significant reduction of this peak after treatment confirms effective dye removal by the GQDs. While Sample B demonstrated strong performance for Cu^{2+} removal, it did not exhibit the lowest absorbance for MB. Instead, Samples D and F showed greater reductions in MB absorbance, indicating higher affinity for dye adsorption. This discrepancy suggests that different GQDs formulations exhibit selective adsorption behaviour towards organic dyes and heavy metal ions, likely due to variations in surface chemistry, functional groups, and particle dispersion. Higher GQDs concentrations (e.g., Sample F) may provide increased available surface area for dye adsorption, despite reduced efficiency for heavy metal removal. Overall, UV–Vis analysis indicates that Sample B exhibits the

https://doi.org/10.24191/jmeche.v23i2.11759

most balanced performance for both heavy metal and dye removal, whereas excessive concentration or inadequate purification negatively affect adsorption efficiency.

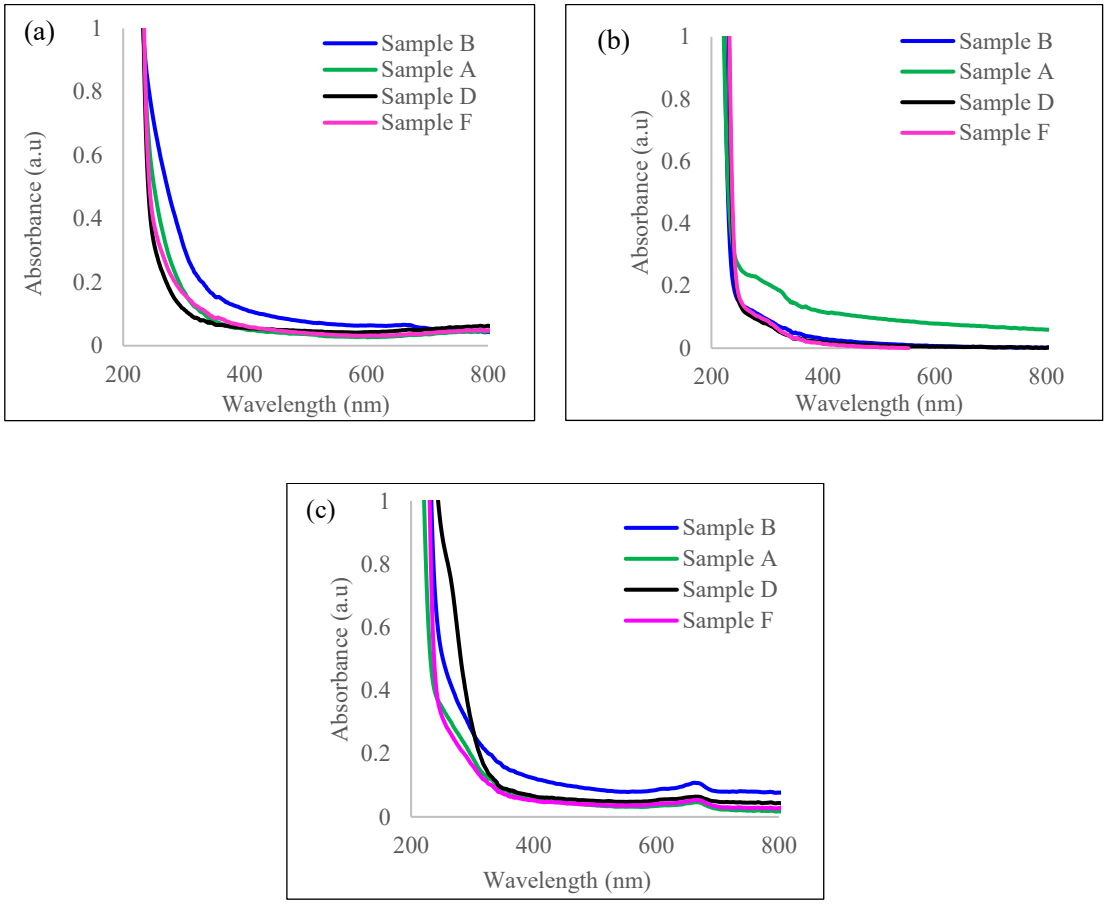

Fig. 8. UV-Vis result for the (a) synthesized GQDs, (b) after mixing with 1.3 mg/L of $CuSO_4$, and (c) after addition of 0.2 mg/L of MB.

Previous studies have demonstrated that GQD-based materials exhibit high adsorption capacities and removal efficiencies for MB. For example, GQDs combined with activated carbon and TiO_2 achieved adsorption capacities of up to 313 mg/g and removal efficiencies exceeding 85–97% under optimized conditions (Tohamy et al., 2023). Similarly, carbon quantum dot-based nanocomposites have demonstrated efficient MB removal, with strong adsorption performance and well-fitting kinetic models (El Ghacham et al., 2025). In comparison, the present study demonstrates effective decolourization of MB at a very low concentration (0.2 mg/L), indicating strong adsorption capability under dilute conditions. However, unlike previous studies, adsorption capacity (mg/g) and removal efficiency (%) were not quantitatively determined, limiting direct numerical comparison.

For heavy metal removal, Li et al. (2022) reported removal efficiencies exceeding 80% for ions such as Cr^{6+} and Pb^{2+} using functionalized GQDs–ZIF-8 composite materials. In this study, Cu^{2+} removal was demonstrated through a significant reduction in EC from 956 µS/cm to 438 µS/cm (~54.2% reduction), confirming effective ion removal. Previous studies have reported that the incorporation of graphene-based

https://doi.org/10.24191/jmeche.v23i2.11759

materials can significantly enhance adsorption performance, where the addition of 20 wt% graphene oxide increased the adsorption capacity for Cu^{2+} by up to 13 times (Serafim et al., 2025). This highlights the strong contribution of oxygen-containing functional groups and high surface area in improving heavy metal ion binding, which supports the observed adsorption behaviour of graphene-based nanomaterials in the present study. Although the adsorption performance in this work is lower than that of engineered GQD-based composites, the present system offers a sustainable, low-cost, and environmentally friendly alternative with promising applicability for low-concentration water treatment.

CONCLUSIONS

In conclusion, this study successfully developed a sustainable and environmentally friendly approach for synthesizing graphene quantum dots (GQDs) from rice husk, an abundant biomass waste, without the use of harsh chemicals. A simple boiling method, combined with deionized water and sonication, effectively converted carbon-rich rice husk into fluorescent GQDs with promising optical and structural properties. The optimal performance was achieved for the 2.5% w/v filtered GQDs (Sample B), which exhibited green fluorescence under UV illumination, a zeta potential of -20.60 ± 1.00 mV indicating good colloidal stability, and a strong photoluminescence emission peak at 513.03 nm upon excitation at 447 nm. Furthermore, this sample demonstrated promising performance in wastewater treatment applications, effectively removing both methylene blue (MB) dye and copper ions from contaminated water. Specifically, the electrical conductivity (EC) of the $CuSO_4$ solution decreased by 54.2%, while the EC of the MB solution increased slightly by 21.5%, likely due to the release of ionic species from the GQDs surface. UV–Vis analysis supported these findings, showing a reduction in the characteristic absorbance peaks of MB and Cu^{2+}, along with visible decolourization of the treated solutions. These results highlight the potential of rice husk-derived GQDs as sustainable nanomaterials for water purification.

For future work, further investigation is required to determine the optimal concentration range for different contaminants. Although higher GQDs concentrations were initially expected to enhance performance, the results indicate that excessive loading may lead to aggregation or surface saturation, thereby reducing adsorption efficiency. Additionally, the performance of GQDs should be evaluated against a broader range of contaminants, including various heavy metals, dyes, and emerging pollutants. Integration of GQDs with other nanomaterials or functional membranes is also recommended to enhance selectivity and overall treatment efficiency.

ACKNOWLEDGEMENTS/ FUNDING

The authors would like to acknowledge the support of the Faculty of Mechanical Engineering, UiTM Shah Alam, Selangor, Malaysia, for providing the technical support for this research. The work was financially funded by the Fundamental Research Grant Scheme (FRGS/1/2025/TK10/U ITM/02/1) of the Ministry of Higher Education Malaysia.

CONFLICT OF INTEREST STATEMENT

The authors agree that this research was conducted in the absence of any self-benefit, commercial, or financial conflicts, and declare the absence of any conflicts of interest with the funders.

https://doi.org/10.24191/jmeche.v23i2.11759

AUTHORS' CONTRIBUTIONS

The authors confirm their contributions to this paper as follows: study conception and design, data collection, and draft manuscript preparation were performed by Faiz Haikal Johari; Azib Hazman carried out material characterization data collection; Siti Rabizah Makhsin conducted analysis and interpretation of results; draft review was performed by Siti Rabizah Makhsin, Syazwani Mohd Zaki and Beenish Siddique; Siti Rabizah Makhsin handled manuscript submission. All authors have approved the final version of the manuscript.

DECLARATION OF GENERATIVE AI IN THE WRITING PROCESS

The authors declare that generative AI and AI-assisted technologies were used in the writing process solely to improve the readability and language quality of this manuscript. These tools were not used to generate scientific content, interpret results, or draw conclusions. The authors take full responsibility for the originality, accuracy, and integrity of the work.

DATA AVAILABILITY/ SUPPLEMENTARY MATERIALS

Available upon request: The datasets used and/or analysed during the current study are available from the corresponding author on reasonable request.

ETHICS STATEMENT

The authors declare that this research did not involve human or animal subjects. All experimental procedures were conducted in accordance with the Safety, Health, and Environmental (HSE) protocols of the Faculty of Mechanical Engineering, Universiti Teknologi MARA (UiTM), Shah Alam, Selangor, Malaysia.

REFERENCES

Boran, F., Çavuş, Ö., Alver, E., & Okutan, M. (2026). Bio-graphene oxide materials from biomass: a green, one-step synthesis via low-temperature combustion. Diamond and Related Materials, 163, 113388.

Bressi, V., Ferlazzo, A., Iannazzo, D., & Espro, C. (2021). Graphene quantum dots by eco-friendly green synthesis for electrochemical sensing: recent advances and future perspectives. Nanomaterials, 11(5), 1120.

Chai, X., He, H., Fan, H., Kang, X., & Song, X. (2019). A hydrothermal-carbonization process for simultaneous production of sugars, graphene quantum dots, and porous carbon from sugarcane bagasse. Bioresource Technology, 282, 142–147.

Cui, Y., Liu, L., Shi, M., Wang, Y., Meng, X., Chen, Y., Huang, Q., & Liu, C. (2024). A review of advances in graphene quantum dots: from preparation and modification methods to application. C, 10(1), 7.

Dong, Y., Shao, J., Chen, C., Li, H., Wang, R., Chi, Y., Lin, X., & Chen, G. (2012). Blue luminescent

graphene quantum dots and graphene oxide prepared by tuning the carbonization degree of citric acid. Carbon, 50(12), 4738–4743.

El Ghacham, S., El Hadj Ali, Y. A., Hejji, L., El Mail, N., Azzouz, A., Chraka, A., Pérez-Villarejo, L., Sánchez-Soto, P. J., Souhail, B., & Sonne, C. (2025). Efficiency of magnetite decorated with carbon quantum dot nanocomposites for the adsorptive removal of methylene blue from wastewater: kinetic and modeling studies. Journal of Molecular Liquids, 424, 127128.

Hong, S., Choi, D. W., Kim, H. N., Park, C. G., Lee, W., & Park, H. H. (2020). Protein-based nanoparticles as drug delivery systems. Pharmaceutics, 12(7), 604.

Li, H., Cheng, Y., Li, J., Li, T., Zhu, J., Deng, W., Zhu, J., & He, D. (2022). Preparation and adsorption performance study of graphene quantum dots@ZIF-8 composites for highly efficient removal of volatile organic compounds. Nanomaterials, 12(22), 4008.

Marie, E., & Torbjorn, W. (2007). Surface analytical techniques applied to cleaning processes. In I. Johansson & P. Somasundaran (Eds.), Handbook for cleaning/decontamination of surfaces (Vol. 2, pp. 747–789). Elsevier.

More, M. P., Lohar, P. H., Patil, A. G., Patil, P. O., & Deshmukh, P. K. (2018). Controlled synthesis of blue luminescent graphene quantum dots from carbonized citric acid: assessment of methodology, stability, and fluorescence in an aqueous environment. Materials Chemistry and Physics, 220, 11–22.

Moresi, M., & Parente, E. (2014). Fermentation (industrial): Production of some organic acids (citric, gluconic, lactic, and propionic). In C. A. Batt & M. L. Tortorello (Eds.), Encyclopedia of food microbiology (2nd Ed., pp. 804–815). Elsevier.

National Research Council. (2000). Copper in drinking water. National Academies Press (US).

Piotrowski, P., Buza, M., Nowaczyński, R., Kongsuwan, N., Surma, H. B., Osewski, P., Gajc, M., Strzep, A., Ryba-Romanowski, W., Hess, O., & Pawlak, D. A. (2024). Ultrafast photoluminescence and multiscale light amplification in nanoplasmonic cavity glass. Nature Communications, 15, 3309.

Rahardjo, S. B., Saraswati, T. E., Masykur, A., Finantrena, N. N. F., & Syaima, H. (2018). Synthesis and characterization of tetrakis(2-amino-3-methylpyridine)copper(II) sulfate tetrahydrate. IOP Conference Series: Materials Science and Engineering, 349, 012056.

Roslan, N. H. I., Makhsin, S. R., Rani, R. A., & Siddique, B. (2025). Effect of gold nanoparticle size conjugated with graphene quantum dots on the signal of a fibre optic sensor. Malaysian Journal of Chemistry, 27(5), 190–199.

Rusli, N. M., Noor, Z. Z., & Taib, S. M. (2024). Life cycle assessment of rice production in Muda Granary Area, Kedah, Malaysia. Journal of Advanced Research in Applied Sciences and Engineering Technology, 35(2), 69–83.

Saleem, H., Saud, A., & Zaidi, S. J. (2023). Sustainable preparation of graphene quantum dots from leaves of date palm tree. ACS Omega, 8(31), 28098–28108.

Serafim, N. B. V., de Araujo, C. M. B., Cavalcanti, J. V. F. L., Ferreira, A. F. P., & da Motta Sobrinho, M. A. (2025). Pb^{2+} and Cu^{2+} removal using graphene oxide-based hydrogel biocomposite as adsorbent: from equilibrium to co-adsorption and mechanism analysis. Journal of Inorganic and Organometallic Polymers and Materials, 1–14.

Shahu, B., Verma, N., Verma, A., Yadav, R., & Khan, S. (2023). Physico-chemical analysis of drinking water. International Journal of Creative Research Thoughts, 11(1), 782–785.

https://doi.org/10.24191/jmeche.v23i2.11759

Shtepliuk, I., Caffrey, N. M., Iakimov, T., Khranovskyy, V., Abrikosov, I. A., & Yakimova, R. (2017). On the interaction of toxic heavy metals (Cd, Hg, Pb) with graphene quantum dots and infinite graphene. Scientific Reports, 7, 3934.

Thakur, T., Kang, M., & Pandey, S. (2026). Revolutionizing wastewater treatment: Breakthroughs in carbon-based nanomaterials. Water remediation methods and wastewater treatment (pp. 953–981). Elsevier.

Tohamy, H. A. S., Fathy, N. A., El-Sakhawy, M., & Kamel, S. (2023). Boosting the adsorption capacity and photocatalytic activity of activated carbon by graphene quantum dots and titanium dioxide. Diamond and Related Materials, 132, 109640.

Yin, X., Liu, L., & Ai, F. (2021). Enhanced photocatalytic degradation of methylene blue by WO_3 nanoparticles under NIR light irradiation. Frontiers in Chemistry, 9, 683765.

Zhu, X., Li, Z., Hu, G., Li, J., & Xiang, B. (2021). The effects of various molecular weight of passivator on the photoluminescence properties of graphene quantum dots. Materials Chemistry and Physics, 258, 123922.

https://doi.org/10.24191/jmeche.v23i2.11759